

From prethermalization to chaos in periodically driven coupled rotors

Yonathan Sadia,^{1,2} Emanuele G. Dalla Torre,^{1,2} and Atanu Rajak³

¹*Department of Physics, Bar-Ilan University, Ramat Gan 5290002, Israel*

²*Center for Quantum Entanglement Science and Technology,
Bar-Ilan University, Ramat Gan 5290002, Israel*

³*Presidency University, Kolkata, West Bengal 700073, India*

Periodically driven (Floquet) systems are said to prethermalize when their energy absorption is very slow for long time. This effect was first discovered in quantum spin models, where the heating rate is exponentially small in the ratio between the driving frequency and the spin bandwidth. Recently, it was shown that prethermalization occurs also in classical systems with an infinite bandwidth. Here, we address the open question of which small parameter controls the lifetime of the prethermal state in these systems. We, first, numerically study the dependence of the lifetime on the initial conditions and on the connectivity in a system of periodically driven coupled rotors. We find that the lifetime is controlled by the temperature of the prethermal state, which is quasi-conserved when the heating is slow. This finding allows us to develop a simple analytical model that describes the crossover from prethermalization to chaos in many-body classical systems.

I. INTRODUCTION

Periodic driving of isolated many-body systems can generate novel dynamical phases that do not have any static analogues. This approach, known as Floquet engineering [1–3], led to a plethora of new phases, such as (anomalous) Floquet topological insulator [4–14] and time crystals [15–21]. However, periodic driving also introduces heating, which hinders such novel applications. The heating can be suppressed by introducing strong disorder in interacting many-body systems, thus creating many-body localized phases [22, 23]. The drawback of this method is that the disorder can destroy the generic characteristics of the non-equilibrium phases. An alternative method that can be used to reduce heating is driving the systems at high frequencies, leading to a long-lived prethermal state, where the heating rate is exponentially slowed down. This phenomenon was first discovered in quantum many-body systems [24–34]. Recently, using quantum simulator [35, 36] and NMR techniques [37], the existence of long-lived prethermal states at high frequency driving has been observed in experiments. The existence of prethermal plateau has also been observed in interacting quantum kicked rotor, realized experimentally in optical lattices [38].

A fundamental question is whether the phenomenon of Floquet prethermalization can be found in classical systems as well. The answer to this question has been given affirmatively in the recent literature [39–44]. Using canonical models of classical chaos theory [40, 43] and classical driven spin chains [41, 42], a quasistationary prethermal regime has been found, before heating begins. In contrast to quantum systems, where Floquet prethermalization rigorously applies to models with bounded operators, classical prethermalization occurs in systems with unbounded spectra and has a statistical nature [40, 43].

The prethermal state of periodically driven classical chaotic systems can be characterized by a generalized Gibbs ensemble (GGE) [43–45]. For example, in the

case of coupled rotors, the total angular momentum is a true conserved quantity, whereas the energy is quasi-conserved inside the prethermal regime. The temperature of the prethermal state can be calculated by equating the energy of the initial ensemble, with the average energy of the GGE. When the ratio between the driving frequency and the temperature is large, the heating rate is suppressed by the low probability for the GGE to satisfy the conditions of a many-body resonance [43], leading to a statistical Floquet prethermalization. In a recent work, the different dynamical regimes of the system were further characterized by considering spatio-temporal correlations [46]. In analogy to the static case [45], these correlations show a diffusive behavior inside the prethermal regime, thus supporting the quasi-static nature of the prethermal state.

In this article, we consider the effect of initial conditions and connectivity of the rotors on the lifetime of the prethermal states. Our main result is that the two effects act in a similar way, namely by affecting the initial energy and, hence, changing the temperature of the prethermal state. First, the effect of initial conditions is investigated by tuning the standard deviation of the angles of the rotors in the initial state. By studying the dependence of the lifetime of the prethermal state on the standard deviation, we establish that the lifetime depends exponentially on the inverse temperature of the prethermal state. Next, we investigate the connectivity of the rotors by considering a many-body kicked rotor model where all the rotors interact with each other. Unlike the nearest-neighbor case, we find that the kinetic energy per rotor, for fixed initial conditions, depends on the number of rotors N , and the prethermal temperature increases linearly with \sqrt{N} . Also in this case, the lifetime varies exponentially as the inverse temperature. Starting from these results, we propose an analytical *ansatz* that describes the universal properties of the crossover from the prethermal regime to the chaotic one.

II. THE MODEL: COUPLED KICKED ROTORS IN ONE AND HIGHER DIMENSIONS

In this work we consider a canonical example of chaotic, classical, many-body systems, namely the coupled kicked rotors Hamiltonian [47–53]

$$H(t) = \sum_{i=1}^N \frac{p_i^2}{2} - \Delta(t) \sum_{i,j=1,i < j}^N \kappa_{i,j} \cos(\phi_i - \phi_j). \quad (1)$$

Here, p_i and ϕ_i are, respectively, the angular momentum and the angle of i -th rotor and N is the total number of rotors. The system is periodically driven with delta-function kicks, $\Delta(t) = \sum_n \delta(t - n\tau)$, where τ is the time period. The couplings $\kappa_{i,j}$ correspond to the interactions between the rotors and define the kick strength. We consider two types of interactions between the rotors: (i) a one-dimensional model with nearest-neighbor coupling, where $\kappa_{i,j} = \kappa(\delta_{i,j-1} + \delta_{i,j+1})$, and (ii) a mean-field model with all-to-all coupling, where $\kappa_{i,j} = \kappa/\sqrt{N}$ [62].

Using Hamilton's equations of motion, one obtains a discrete map of p_i and ϕ_i between consecutive kicks,

$$\begin{aligned} p_i(t + \tau) &= p_i(t) - \sum_{j \neq i} \kappa_{i,j} \sin(\phi_i - \phi_j), \\ \phi_i(t + \tau) &= \phi_i(t) + p_i(t + \tau)\tau. \end{aligned} \quad (2)$$

These equations are a many-body generalization of Chirikov standard map [54], a system of paramount importance for the study of the transition between regular and chaotic dynamics. By rescaling $p_i \rightarrow p_i\tau$, one finds that the equations of motion (2) are characterized by a single dimensionless parameter, $K = \kappa\tau$. Hence, in what follows, we will set $\tau = 1$ without loss of generality. As we will see, the initial conditions and the connectivity introduce additional unitless parameters that can be used to tune the prethermal regime.

Because the model (1) is non-integrable, at long times it shows a chaotic behavior, where the kinetic energy $E_{\text{kin},i}(t) = \langle p_i^2 \rangle / 2$ grows linearly with time, $E_{\text{kin},i}(t) \approx \Gamma t$ [63]. The heating rate Γ can be estimated using the following approach: According to Eqs. (2), the momentum at time t equals to

$$p_i(t) = p_i(0) - \sum_{n=0}^{t-1} \sum_{j \neq i} \kappa_{i,j} \sin(\phi_i(n) - \phi_j(n)) \quad (3)$$

Now, squaring Eq. (3) and averaging over symmetric initial conditions with $\langle p_i(0) \rangle = 0$, we obtain

$$\begin{aligned} \langle p_i^2(t) \rangle &= \langle p_i^2(0) \rangle + \\ &\sum_{m,n=0}^{t-1} \sum_{j,k \neq i} \kappa_{i,j} \kappa_{i,k} \left\langle \sin(\phi_i(m) - \phi_j(m)) \sin(\phi_i(n) - \phi_k(n)) \right\rangle. \end{aligned} \quad (4)$$

In the chaotic regime, the angles of the rotors become statistically uncorrelated both in space and time, and we can

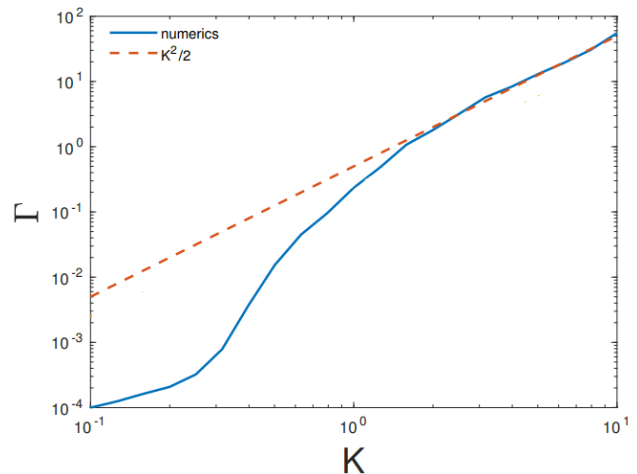


FIG. 1: Heating rate for one-dimensional model, as a function of the coupling parameter K . For large K , it follows the relation $K^2/2$.

approximate $\langle \sin(\phi_i(m) - \phi_j(m)) \sin(\phi_i(n) - \phi_k(n)) \rangle = \delta_{j,k} \delta_{m,n} / 2$

For the one-dimensional model, only the terms $j = k = i \pm 1$ contribute to the sum of Eq. (4), leading to $\langle p_i^2 \rangle = K^2 t$, or equivalently $\Gamma = K^2/2$. From the comparison with numerical simulations of the model, it was found that our analytical result for the heating rate is valid for large K (see Fig. 1). For small K , the rotors move in a correlated way and, for $K \lesssim 0.1$ the heating is approximately given by $\Gamma \approx 10K^{6.5}$ [49, 50, 52]. This effect, known as “fast Arnold diffusion” was explained in Refs. [50, 55] using the concept of many-body resonance [47]. Importantly, for all values of K , the heating rate does not depend on N [64].

In the case of all-to-all coupling, all terms with $j = k \neq i$ equally contribute to Eq. (4) and one obtains $\langle p_i^2(t) \rangle = (N-1)\kappa^2/(2N)t$. For large N , the heating rate, $\Gamma \approx K^2/4$, becomes independent on N . To verify the validity of the uncorrelated behavior of the rotors in the heating regime, we numerically compute the dynamics of the system for long times and compute the heating rate in the chaotic regime, see Fig. 2. For small values of the coupling parameter, say $K = 0.15, 0.3$, we find that Γ increases with N and saturates to a value $K^2/8$ for large N (see Fig. 2(a)), whereas the theoretically expected value is $K^2/4$. This anomaly is resolved by plotting Γ as a function of N for large K . From Fig. 2(b), we see that the heating rate saturates to a value closer to $K^2/4$ for large N with a large K , i.e., when the system is well inside the chaotic regime.

These results indicate that in both models, our assumption of an uncorrelated behavior of the angles is valid for large values of K only. For small values of K the rotors undergo a correlated dynamics, even in the diffusive long-time limit. Importantly, our simulations demonstrate that for all values of K , in both models the heating rate does not depend on N for large enough N .

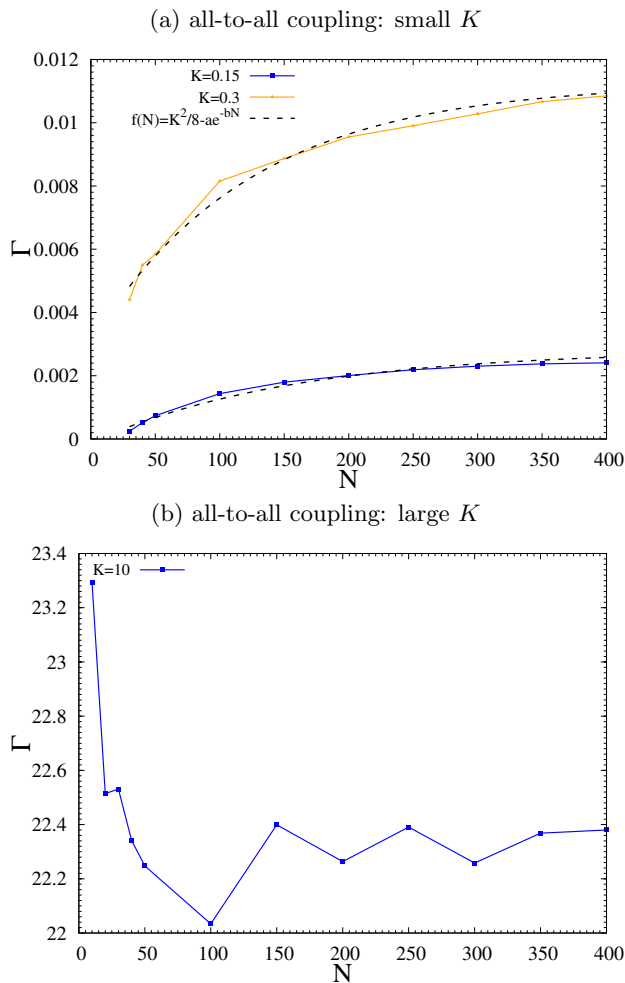


FIG. 2: Heating rate as a function of N of all-to-all coupling model for (a) small values of K and (b) a large value of K .

III. ENERGY AND TEMPERATURE IN THE PRETHERMAL STATE

We open our discussion by considering the prethermal regime, shortly after the initial conditions. In systems displaying statistical Floquet prethermalization, the time-averaged Hamiltonian H_{av} is quasi-conserved. Here,

$$H_{\text{av}} = \frac{1}{\tau} \int_0^\tau dt H(t) = \sum_{i=1}^N \frac{p_i^2}{2} - \sum_{i<j}^N \frac{\kappa_{ij}}{\tau} \cos(\phi_i - \phi_j). \quad (5)$$

At short times, we can assume that the average energy in the prethermal state equals to the average energy in the initial state

$$\langle H_{\text{av}} \rangle_T = \langle H_{\text{av}} \rangle_0, \quad (6)$$

where $\langle \dots \rangle_T$ is the Boltzmann distribution with Hamiltonian H_{av} and temperature T , and $\langle \dots \rangle_0$ is the average over the initial conditions. This equation can be used

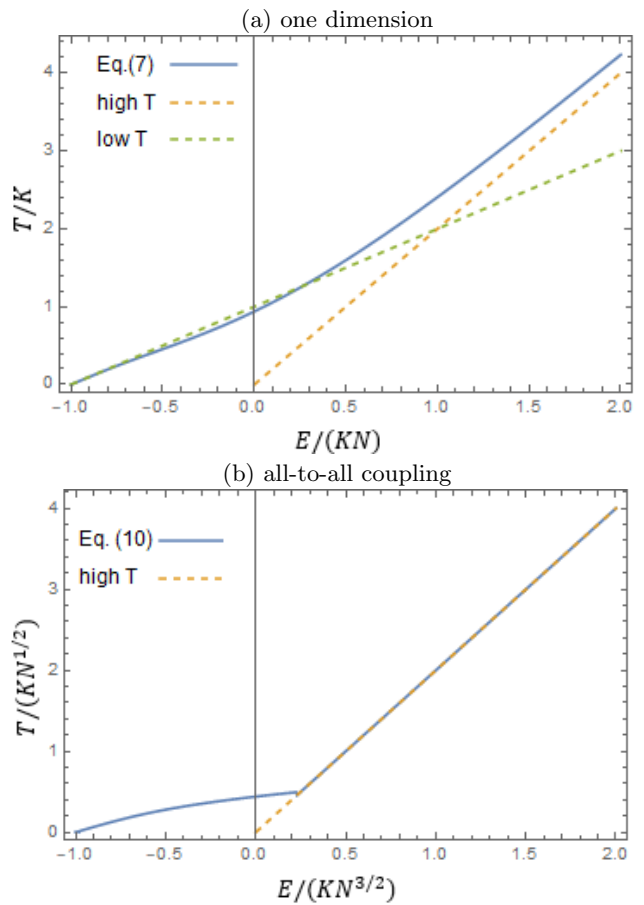


FIG. 3: Temperature as a function of the energy $E = \langle H_{\text{av}} \rangle$ for (a) the one dimensional model and (b) the all-to-all coupling model, obtained by the numerical solution of Eq. (7) and (10), respectively. The dashed lines are asymptotic results at small and large energies (see text).

to derive the temperature of the prethermal state from a given set of initial conditions.

Let us, first, consider the one dimensional model, where the thermal average can be performed exactly [43] and leads to

$$\frac{\langle H_{\text{av}} \rangle_T}{N} = \frac{T}{2} - K \frac{I_1(K/T)}{I_0(K/T)} \quad (7)$$

Here, the right-hand side corresponds to the sum of the kinetic energy per rotor, $T/2$, and the potential energy per rotor, expressed in terms of the modified Bessel functions I_0 and I_1 . The numerical solution of this equation is shown in Fig. 3(a). At large temperatures, $T \gg K$, we can neglect the potential energy and obtain $\langle H_{\text{av}} \rangle_T = NT/2$. In the opposite limit, $T \ll K$, we find $\langle H_{\text{av}} \rangle = N(T - K)$. This result can be understood by observing that at small temperatures we can approximate $\cos(\phi) \approx 1 - \phi^2/2$, leading to a set of harmonic oscillators, with average potential energy $-K + T/2$. The situation studied in Ref. [43] corresponds to the case $E = 0$, where $T = 0.9384K$.

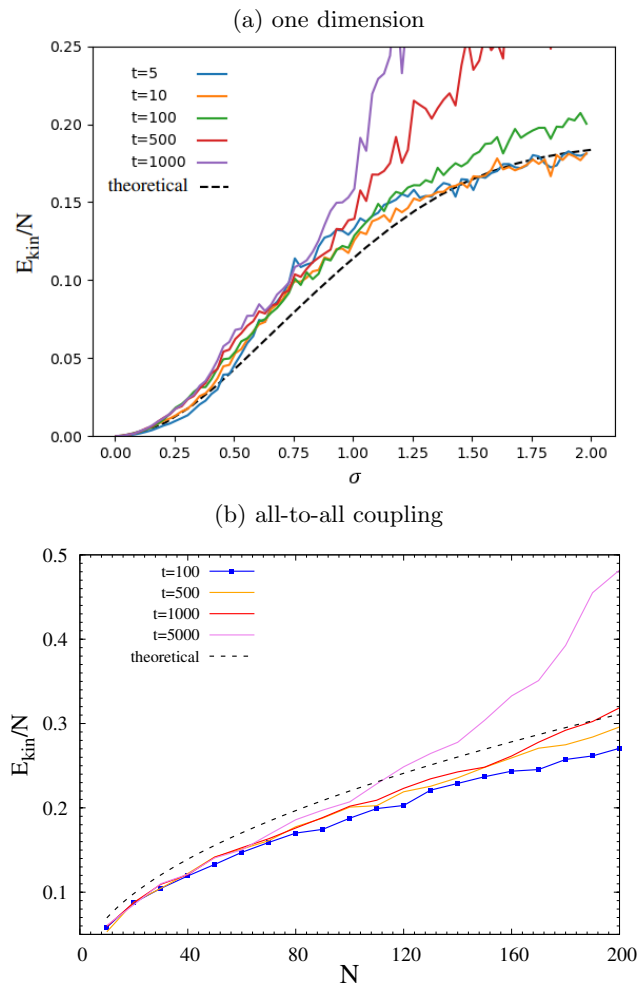


FIG. 4: Kinetic energy per rotor in the prethermal state: (a) in the one-dimensional model for $K = 0.4$, as a function of the initial fluctuations σ ; (b) in the all-to-all coupling model for $K = 0.1$, as a function of the number of rotors N . The dashed lines are our analytical predictions (see text for details).

In our numerical simulations we consider $p_i(t=0) = 0$ and extract $\phi_i(t=0)$ from a Gaussian distribution with standard deviation σ . In this case, the initial energy is

$$\frac{\langle H_{\text{av}} \rangle_0}{N} = -K e^{-\sigma^2}, \quad (8)$$

The free parameter σ controls the temperature of the initial state and, consequently, the energy of the prethermal state. By equating Eq. (8) and Eq. (7), we find an implicit relation between the parameter σ and the temperature of the prethermal state. In Fig. 4(a) we show that the predicted kinetic energy $E_{\text{kin}}/N = T/2$ exactly matches the numerical solution of the model. For $\sigma \rightarrow \infty$, we recover the result of Ref. [43] $T = 0.9384K$.

In the case of all-to-all coupling, the dependence between the energy and the temperature can be computed

within a mean-field approximation [51]

$$\sum_j \cos(\phi_i - \phi_j) \approx N(\langle \cos \phi \rangle \cos \phi_i + \langle \sin \phi \rangle \sin \phi_i), \quad (9)$$

such that

$$\frac{\langle H_{\text{av}} \rangle_T}{N} = \frac{T}{2} - \frac{\kappa}{2\tau} N^{1/2} (\langle \cos \phi \rangle^2 + \langle \sin \phi \rangle^2), \quad (10)$$

with

$$\langle \cos \phi \rangle = \langle \sin \phi \rangle = \frac{I_1(c)}{I_0(c)} \quad \text{and} \quad c = \frac{K\sqrt{N}}{2T} \langle \cos \phi \rangle.$$

The last line corresponds to a Boltzmann average over the Hamiltonian H_{av} , with the approximation (9). Note that Eq. (10) is a function of the rescaled parameters $E/(KN^{3/2})$ and $T/(K\sqrt{N})$ only. The numerical solution of this equation is shown in Fig. 3(b). At high temperatures $\langle \cos \phi \rangle = 0$ and one simply has $E = NT/2$ (the potential energy becomes negligible). In our numerical simulations the rotors are initialized at random angle between 0 and 2π , with $p_i(t=0) = 0$, such that the initial energy is $\langle H_{\text{av}} \rangle_0 = 0$ and the temperature of the prethermal state is $T = 0.44K\sqrt{N}$, see Fig. 4(b). Hence, in the all-to-all coupling model the initial energy and the temperature of the prethermal state are controlled by N .

IV. FROM PRETHERMALIZATION TO CHAOS

A. Numerics in one dimension

We now focus on the transition between the prethermal state and the chaotic regime, starting from the one-dimensional model. Figure 5 shows the time evolution of the kinetic energy per rotor for different values of the initial fluctuations' parameter σ . Note that, in this plot, the transition between the prethermal and chaotic regimes appear to become sharper with decreasing σ . This is inconsistent with the normalization procedure proposed by Ref. [40], $t \rightarrow t/t^*$, which corresponds to a rigid shift in the logarithmic scale. Interestingly, we observed that the curves collapse over many orders of magnitude, when a rigid shifted is applied on a linear scale, $t \rightarrow t - t^*$. To demonstrate this effect, in Fig. 6 we define t^* by $E_{\text{kin}}(t^*)/N = 1$ and plot $E_{\text{kin}}(t - t^*)$, obtaining a perfect data-collapse for both $t < t^*$ and $t > t^*$. In Fig. 7 we show the dependence of t^* on the inverse temperature of the prethermal state and find an exponential behavior. These numerical findings will be explained by the analytical model developed in Sec. IV C.

B. Numerics of all-to-all coupling

We now move to the case of all-to-all coupling. In Sec. II, we used a mean-field theory to compute the heating rate in the chaotic regime and demonstrated that it

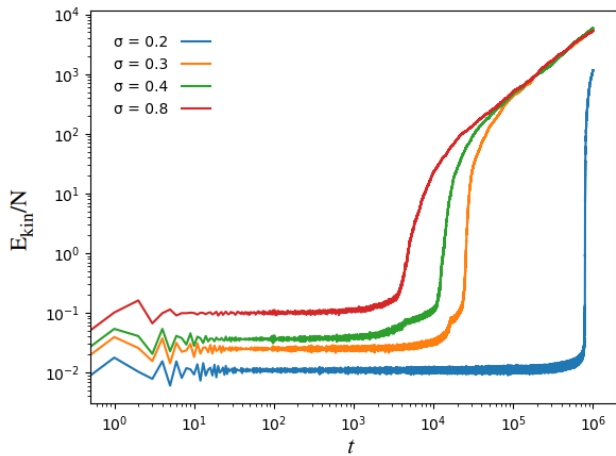


FIG. 5: Time evolution of the kinetic energy for the one-dimensional model ($K = 0.4$), for different values of the standard deviation of initial angles, σ . As shown in Fig. 6, all the curves correspond to the same function, shifted in the time axis. The apparent change of the slope is an artifact of the logarithmic scale.

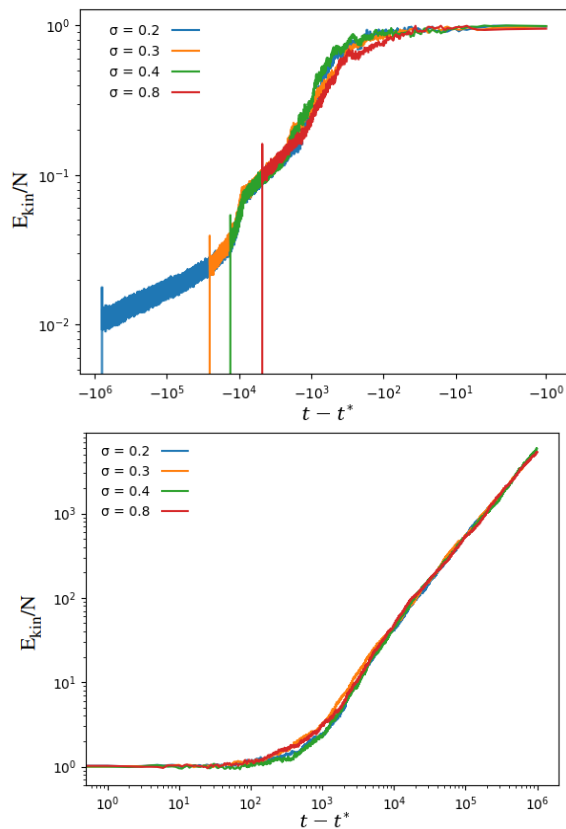


FIG. 6: Same curves as Fig. 5, plotted as a function of $t^* - t$, for $t < t^*$ (upper panel), and $t - t^*$ for $t > t^*$ (lower panel). The excellent data collapse demonstrates that the transition from the prethermal regime to the chaotic regime is universal and does not depend on the initial conditions.

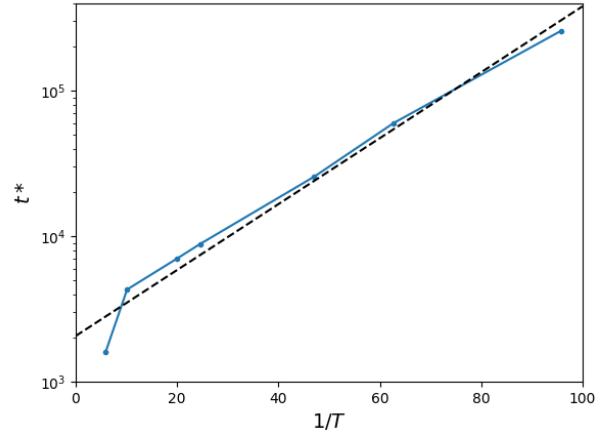


FIG. 7: Lifetime of the prethermal state of the one-dimensional model with $K = 0.4$, as a function of the inverse temperature of the prethermal state $1/T$, obtained by varying σ . The lifetime is exponentially large in the inverse temperature.

does not depend on number of rotors N . In Sec. III we showed that the temperature of the prethermal state increases as $T = 0.44K\sqrt{N}$. Hence, we expect that as we increase N , the lifetime of the prethermal state should decrease. This behavior is indeed observed in the numerical solution of the model, see Fig. 8. To explore this effect in a quantitative manner, we plot the lifetime of the prethermal states (defined by $E_{\text{kin}}(t^*)/N = 1$), as a function of the inverse temperature, and observe two distinct regimes: (i) small inverse temperatures $1/T < 2.5$, corresponding to large number of rotors $N > (0.4/0.44K)^2 \approx 36$; (ii) large inverse temperatures $1/T > 2.5$, corresponding to small number of rotors ($N < 36$). In the former regime, the heating rate is approximately constant and we observe an exponential suppression of heating. In the latter, finite-size effects are significant (see Fig. 2) and cause a further suppression of heating.

C. Effective analytic description

We now present a simple model that describes the escape from the prethermal regime to the chaotic one. The key assumption of the model is that, due to the exponentially slow absorption of energy, the prethermal state is a quasi-equilibrium state, characterized by an instantaneous temperature $T(t)$. We consider the generic situation where the energy absorption depends exponentially on the temperature as

$$\frac{dE(t)}{dt} = NT e^{-A/T(t)} \quad (11)$$

Here $\Gamma = \Gamma(K)$ is the heating rate in the high-temperature, chaotic regime, where $dE/dt = NT$. In

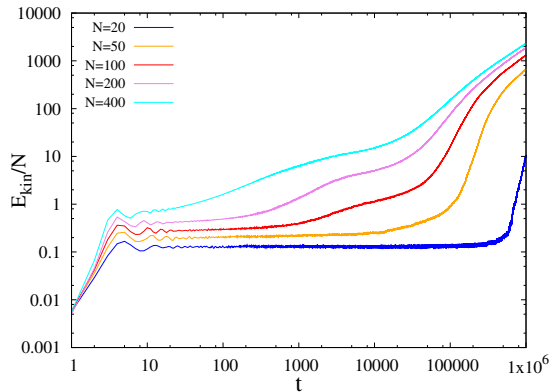


FIG. 8: Time-evolution of the kinetic energy per rotor for the all-to-all coupling with $K = 0.15$, for different values of the number of rotors N . The number of rotors affects the temperature of the prethermal state and its lifetime, while the heating rate in the chaotic regime remains constant.

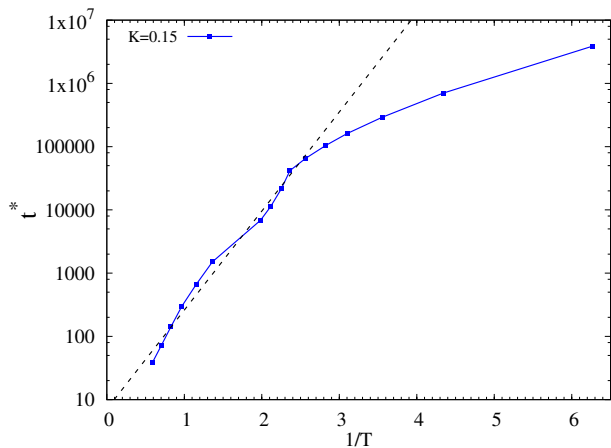


FIG. 9: Lifetime of the prethermal state for the all-to-all coupling with $K = 0.15$, as a function of the inverse temperature of the prethermal state. The temperature T is calculated numerically by $T = 2E_{\text{kin}}/N$, where E_{kin} is the kinetic energy in the prethermal state and T is varied by changing N between 10 and 400. The dashed line is an exponential fit of the large temperature regime (see text).

models of kicked rotors, this exponential suppression of heating is due to the low probability to find a rotor with angular momentum $p_i \sim \Omega = 2\pi/\tau$ in a Boltzmann-Gibbs distribution with temperature $T(t) \ll K$ [43]. See also Ref. [44] for the case of the Bose-Hubbard model, where the exponential suppression is associated to the low probability to find sites with large occupation numbers.

In order to solve Eq. (11), we need to combine the energy-temperature relation $T = T(E)$. As shown in Sec. III, this relation is often linear. For simplicity, we use here the high-temperature result $T = 2E/N$, such

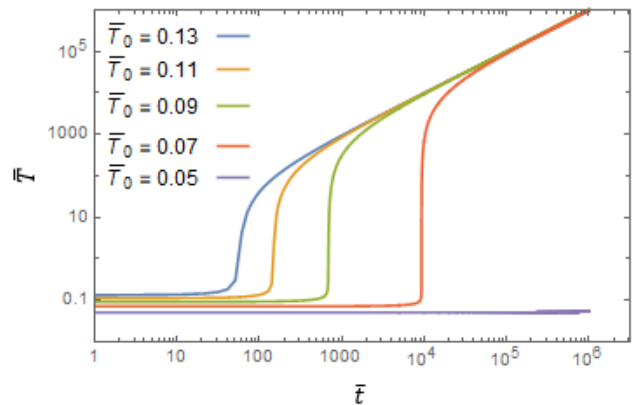


FIG. 10: Time evolution of the temperature, obtained by the numerical solution of the rescaled analytical model, Eq. (13), for different initial conditions. The dashed lines are the lifetimes of the prethermal state predicted by Eq. (15).

that

$$\frac{dT}{dt} = 2\Gamma e^{-A/T(t)} \quad (12)$$

At short times, $T(t) \approx (T_0 + 2\Gamma e^{-A/T_0} dt)$ and the energy absorption is exponentially suppressed, leading to a long-lived prethermal regime. In contrast, at long times $T(t) \approx 2\Gamma t$, corresponding to the chaotic regime. Equation (12) offers the minimal model of statistical prethermalization, where an exponentially long prethermal regime, is followed by a chaotic regime with linearly increasing temperature.

To compute the solution at intermediate times, it is useful to introduce the rescaled temperatures $\bar{T} = T/A$ and time $\bar{t} = 2\Gamma t/A$, satisfying

$$\frac{d\bar{T}}{d\bar{t}} = e^{-1/\bar{T}}. \quad (13)$$

This equation has an implicit solution in terms of incomplete Gamma functions, shown in Fig. (10) for different values of $\bar{T}(0)$. Note that all the curves are identical, up to a shift in the \bar{t} axis and the increasing sharpness for decreasing \bar{T}_0 is an artifact of the logarithmic scale (see Sect. IV A).

We can evaluate the lifetime of the prethermal, by computing the time at which the curve reaches some target value. This is equivalent to solving the inverse of Eq. (13), namely

$$t^* = \int_{\bar{T}_0}^1 d\bar{T} e^{1/\bar{T}} \quad (14)$$

Here we have set the upper limit to $\bar{T} = 1$, such that t^* is defined as the time required to reach $\bar{T}(t^*) = 1$. The integral in Eq. (14) is readily solved to deliver

$$t^* = \text{Ei}\left(\frac{1}{\bar{T}_0}\right) - \bar{T}_0 \exp\left(\frac{1}{\bar{T}_0}\right) - \text{Ei}(1) + e, \quad (15)$$

where Ei is an exponential integral function. For large x , one has $Ei(x) \approx (1/x + 1/x^2)e^x$, leading to

$$t^* = \bar{T}_0^2 \exp\left(\frac{1}{\bar{T}_0}\right). \quad (16)$$

This result shows that the lifetime of the prethermal time depends exponentially upon the inverse temperature of the state itself, as seen in our numerical solution of the one dimensional and all-to-all coupling models.

V. CONCLUSION

In conclusion, we performed a detailed study of the transition from prethermalization to chaos in classical periodically driven systems. We considered two tuning parameters that affect the temperature of the prethermal state, without changing the heating rate. The role of initial conditions is studied by a one-dimensional model where the temperature is set by the standard deviation of the initial Gaussian distribution of the angles. The effect of connectivity is studied by a system where all the rotors interact with each other and the temperature is a function of the number of rotors. In both cases, we computed the lifetime of the prethermal state and found that it depends exponentially on the inverse of the prethermal temperature. We repeated the same calculations in two and three dimensional lattice (not reported here), delivering similar results.

Starting from these numerical results, we proposed a simple model that describes the transition between prethermalization and chaos. Our model relies on two intertwined assumptions, namely that the prethermal state is fully described by its instantaneous temperature and that the heating rate is exponentially suppressed at low temperatures. The analytical solution of the resulting differential equation shows the same qualitative behavior as the numerical calculations. In particular, the lifetime of the prethermal state depends exponentially on the initial temperature of the prethermal state, see Eq. (16). In addition, our analytical model predicts that the curves for different initial conditions can be collapsed by a rigid shift in the time domain, as indeed observed numerically.

Our work rises several questions related to the relation between statistical Floquet prethermalization and other fundamental properties of chaotic systems. The exponential scaling of the heating rate has some similarity with the phenomenon of Arnol'd diffusion, characteristic of systems close to integrability. In these systems, according to the Nekhoroshev theorem, the diffusion rate is bounded by an exponential function of $1/\epsilon^b$, where ϵ is the perturbation from integrability and b depends on the system size [56]. In spite of the similarity between the Nekhoroshev bound and the present study, there are two important differences. First, in the limit of an infinite system, the Nekhoroshev bound is trivially satisfied, while the present effect survives in the limit of $N \rightarrow \infty$. Second, Arnol'd diffusion is valid in the entire phase space, while statistical prethermalization occurs only for initial conditions that correspond to low prethermal temperatures.

As mentioned in the introduction, discrete time crystals are novel non-equilibrium phases that do not have any static analogues. These phases can be observed when the time-translation symmetry of the periodically driven systems is broken spontaneously. Time crystals were, first, predicted theoretically in driven quantum systems and, later, observed in experiments [17, 57]. Recently, a prethermal time crystal has been observed in a quantum simulator experiment with high frequency drive [36]. In parallel, signatures of discrete time-crystals have been found in classical systems [58, 59]. An interesting question for future study is whether classical time crystals can be protected by statistical Floquet prethermalization [60, 61].

VI. ACKNOWLEDGEMENTS

We acknowledge useful discussions with Itzhack Dana and Roberta Citro. AR would like to thank the department of physics of Bar-Ilan University for computational facilities. This work was supported by the Israel Science Foundation, Grants No. 151/19 and 154/19. AR acknowledges UGC, India for start-up research grant F. 30-509/2020(BSR).

-
- [1] T. Oka and S. Kitamura. Floquet engineering of quantum materials. *Annual Review of Condensed Matter Physics*, 10, 387 (2019).
 - [2] M. S. Rudner and N. H. Lindner. Band structure engineering and non-equilibrium dynamics in Floquet topological insulators. *Nature reviews physics*, 2, 229 (2020).
 - [3] C. Weitenberg and J. Simonet. Tailoring quantum gases by Floquet engineering. *arXiv preprint arXiv:2102.07009* (2021).
 - [4] T. Oka and H. Aoki. Photovoltaic Hall effect in graphene. *Physical Review B*, 79, 081406 (2009).
 - [5] N. H. Lindner, G. Refael, and V. Galitski. Floquet topological insulator in semiconductor quantum wells. *Nature Physics*, 7, 490 (2011).
 - [6] M. C. Rechtsman, J. M. Zeuner, Y. Plotnik, et al. Photonic Floquet topological insulators. *Nature*, 496, 196 (2013).
 - [7] Y. T. Katan and D. Podolsky. Modulated Floquet topological insulators. *Physical review letters*, 110, 016802 (2013).
 - [8] G. Jotzu, M. Messer, R. Desbuquois, et al. Experimental realization of the topological Haldane model with ultra-

- cold fermions. *Nature*, 515, 237 (2014).
- [9] R. Fleury, A. B. Khanikaev, and A. Alu. Floquet topological insulators for sound. *Nature communications*, 7, 1 (2016).
- [10] Y.-G. Peng, C.-Z. Qin, D.-G. Zhao, et al. Experimental demonstration of anomalous Floquet topological insulator for sound. *Nature communications*, 7, 1 (2016).
- [11] R. Roy and F. Harper. Periodic table for Floquet topological insulators. *Physical Review B*, 96, 155118 (2017).
- [12] L. J. Maczewsky, J. M. Zeuner, S. Nolte, et al. Observation of photonic anomalous Floquet topological insulators. *Nature communications*, 8, 13756 (2017).
- [13] K. Wintersperger, C. Braun, F. N. Ünal, et al. Realization of an anomalous Floquet topological system with ultracold atoms. *Nature Physics*, 16, 1058 (2020).
- [14] S. Mukherjee and M. C. Rechtsman. Observation of Floquet solitons in a topological bandgap. *Science*, 368, 856 (2020).
- [15] V. Khemani, A. Lazarides, R. Moessner, et al. Phase structure of driven quantum systems. *Physical Review Letters*, 116, 250401 (2016).
- [16] D. V. Else, B. Bauer, and C. Nayak. Floquet time crystals. *Physical Review Letters*, 117, 090402 (2016).
- [17] J. Zhang, P. Hess, A. Kyprianidis, et al. Observation of a discrete time crystal. *Nature*, 543, 217 (2017).
- [18] N. Y. Yao, A. C. Potter, I.-D. Potirniche, et al. Discrete time crystals: rigidity, criticality, and realizations. *Physical Review Letters*, 118, 030401 (2017).
- [19] A. Russomanno, F. Iemini, M. Dalmonte, et al. Floquet time crystal in the Lipkin-Meshkov-Glick model. *Physical Review B*, 95, 214307 (2017).
- [20] R. Moessner and S. Sondhi. Equilibration and order in quantum Floquet matter. *Nature Physics*, 13, 424 (2017).
- [21] J. Rovny, R. L. Blum, and S. E. Barrett. Observation of discrete-time-crystal signatures in an ordered dipolar many-body system. *Physical review letters*, 120, 180603 (2018).
- [22] P. Ponte, Z. Papić, F. Huveneers, et al. Many-body localization in periodically driven systems. *Physical Review Letters*, 114, 140401 (2015).
- [23] A. Lazarides, A. Das, and R. Moessner. Fate of many-body localization under periodic driving. *Physical Review Letters*, 115, 030402 (2015).
- [24] S. Choudhury and E. J. Mueller. Stability of a Floquet Bose-Einstein condensate in a one-dimensional optical lattice. *Physical Review A*, 90, 013621 (2014).
- [25] M. Bukov, S. Gopalakrishnan, M. Knap, et al. Prethermal Floquet steady states and instabilities in the periodically driven, weakly interacting Bose-hubbard model. *Physical Review Letters*, 115, 205301 (2015).
- [26] N. Goldman, J. Dalibard, M. Aidelsburger, et al. Periodically driven quantum matter: The case of resonant modulations. *Physical Review A*, 91, 033632 (2015).
- [27] A. Chandran and S. L. Sondhi. Interaction-stabilized steady states in the driven $O(N)$ model. *Physical Review B*, 93, 174305 (2016).
- [28] S. Lellouch, M. Bukov, E. Demler, et al. Parametric Instability Rates in Periodically Driven Band Systems. *Physical Review X*, 7, 021015 (2017).
- [29] S. Lellouch and N. Goldman. Parametric instabilities in resonantly-driven Bose-Einstein condensates. *Quantum Science and Technology*, 3, 024011 (2018).
- [30] D. A. Abanin, W. De Roeck, and F. Huveneers. Exponentially slow heating in periodically driven many-body systems. *Physical Review Letters*, 115, 256803 (2015).
- [31] T. Kuwahara, T. Mori, and K. Saito. Floquet-Magnus theory and generic transient dynamics in periodically driven many-body quantum systems. *Annals of Physics*, 367, 96 (2016).
- [32] T. Mori, T. Kuwahara, and K. Saito. Rigorous bound on energy absorption and generic relaxation in periodically driven quantum systems. *Physical Review Letters*, 116, 120401 (2016).
- [33] D. Abanin, W. De Roeck, W. W. Ho, et al. A rigorous theory of many-body prethermalization for periodically driven and closed quantum systems. *Communications in Mathematical Physics*, 354, 809 (2017).
- [34] T. Gulden, E. Berg, M. S. Rudner, et al. Exponentially long lifetime of universal quasi-steady states in topological Floquet pumps. *SciPost Physics*, 9 (2020).
- [35] A. Rubio-Abadal, M. Ippoliti, S. Hollerith, et al. Floquet prethermalization in a Bose-Hubbard system. *Physical Review X*, 10, 021044 (2020).
- [36] A. Kyprianidis, F. Machado, W. Morong, et al. Observation of a prethermal discrete time crystal (2021).
- [37] P. Peng, C. Yin, X. Huang, et al. Floquet prethermalization in dipolar spin chains. *Nature Physics*, pages 1–4 (2021).
- [38] A. Cao, R. Sajjad, H. Mas, et al. Prethermal Dynamical Localization and the Emergence of Chaos in a Kicked Interacting Quantum Gas. *arXiv preprint arXiv:2106.09698* (2021).
- [39] R. Citro, E. Dalla Torre, L. D'Alessio, et al. Dynamical stability of a many-body Kapitza pendulum. *Annals of Physics*, 360, 694 (2015).
- [40] A. Rajak, R. Citro, and E. Dalla Torre. Stability and prethermalization in chains of classical kicked rotors. *Journal of Physics A: Mathematical and General*, 51, 465001 (2018).
- [41] O. Howell, P. Weinberg, D. Sels, et al. Asymptotic Prethermalization in Periodically Driven Classical Spin Chains. *Physical Review Letters*, 122, 010602 (2019).
- [42] T. Mori. Floquet prethermalization in periodically driven classical spin systems. *Physical Review B*, 98, 104303 (2018).
- [43] A. Rajak, I. Dana, and E. G. Dalla Torre. Characterizations of prethermal states in periodically driven many-body systems with unbounded chaotic diffusion. *Physical Review B*, 100, 100302 (2019).
- [44] E. G. D. Torre and D. Dentelski. Statistical Floquet prethermalization of the Bose-Hubbard model (2021).
- [45] A. Das, K. Damle, A. Dhar, et al. Nonlinear fluctuating hydrodynamics for the classical XXZ spin chain. *Journal of Statistical Physics*, 180, 238 (2020).
- [46] A. Kundu, A. Rajak, and T. Nag. Dynamics of fluctuation correlation in periodically driven classical system. *arXiv preprint arXiv:2102.12622* (2021).
- [47] B. V. Chirikov. A universal instability of many-dimensional oscillator systems. *Physics Reports*, 52, 263 (1979).
- [48] K. Kaneko and T. Konishi. Diffusion in Hamiltonian dynamical systems with many degrees of freedom. *Physical Review A*, 40, 6130 (1989).
- [49] T. Konishi and K. Kaneko. Diffusion in Hamiltonian chaos and its size dependence. *Journal of Physics A: Mathematical and General*, 23, L715 (1990).
- [50] B. Chirikov and V. Vecheslavov. Theory of fast Arnold

- diffusion in many-frequency systems. *Journal of statistical physics*, 71, 243 (1993).
- [51] M. Antoni and S. Ruffo. Clustering and relaxation in Hamiltonian long-range dynamics. *Physical Review E*, 52, 2361 (1995).
- [52] M. Mulansky, K. Ahnert, A. Pikovsky, et al. Strong and weak chaos in weakly nonintegrable many-body Hamiltonian systems. *Journal of Statistical Physics*, 145, 1256 (2011).
- [53] A. Rajak and I. Dana. Stability, isolated chaos, and superdiffusion in nonequilibrium many-body interacting systems. *Physical Review E*, 102, 062120 (2020).
- [54] B. Chirikov and D. Shepelyansky. Chirikov standard map. *Scholarpedia*, 3, 3550 (2008).
- [55] B. Chirikov and V. Vecheslavov. Arnol'd diffusion in large systems. *Journal of Experimental and Theoretical Physics*, 85, 616 (1997).
- [56] N. Nekhoroshev. An exponential estimate of stability time in Hamiltonian systems close to integrable. *Uspekhi Matematicheskikh Nauk*, 32, 5 (1977).
- [57] S. Choi, J. Choi, R. Landig, et al. Observation of discrete time-crystalline order in a disordered dipolar many-body system. *Nature*, 543, 221 (2017).
- [58] A. Shapere and F. Wilczek. Classical time crystals. *Physical review letters*, 109, 160402 (2012).
- [59] N. Y. Yao, C. Nayak, L. Balents, et al. Classical discrete time crystals. *Nature Physics*, 16, 438 (2020).
- [60] A. Pizzi, A. Nunnenkamp, and J. Knolle. (Classical) Prethermal phases of matter. *arXiv preprint arXiv:2104.13928* (2021).
- [61] A. Pizzi, A. Nunnenkamp, and J. Knolle. (Classical) Prethermal phases of matter in dimension 1, 2, and 3. *arXiv preprint arXiv:2108.07272* (2021).
- [62] The normalization of the latter model is discussed below.
- [63] The heating rate Γ is related to the diffusion coefficient D , defined as $\langle p_i^2 \rangle = Dt$, by $\Gamma = D/2$
- [64] see Appendix B of Ref. [40]